JACS
JOURNAL OF THE AMERICAN CHEMICAL SOCIETY

Communication

pubs.acs.org/JACS

Transformable Nanostructures of Platinum-Containing Organosilane Hybrids: Non-covalent Self-Assembly of Polyhedral Oligomeric Silsesquioxanes Assisted by Pt···Pt and $\pi-\pi$ Stacking Interactions of Alkynylplatinum(II) Terpyridine Moieties

Ho-Leung Au-Yeung, Sammual Yu-Lut Leung, Anthony Yiu-Yan Tam, and Vivian Wing-Wah Yam*

Institute of Molecular Functional Materials (Areas of Excellence Scheme, University Grants Committee (Hong Kong)), and Department of Chemistry, The University of Hong Kong Pokfulam Road, Hong Kong

Supporting Information

ABSTRACT: An alkynylplatinum(II) terpyridine complex functionalized with polyhedral oligomeric silsesquioxanes (POSS) moieties has been demonstrated to exhibit self-association behavior to give various distinguishable nanostructures with interesting morphological transformation from rings to rods in response to solvent conditions through the stabilization of Pt···Pt and $\pi-\pi$ stacking interactions as well as hydrophobic−hydrophobic interactions. These changes can be systemically controlled by varying the solvent composition and have been studied by ^{1}H NMR, electron microscopy, UV−vis absorption, and emission spectroscopies.

Platinum(II) polypyridine complexes of d^8 square-planar configuration have aroused much attention and have been increasingly investigated owing to their intriguing spectroscopic and luminescent properties as well as their propensity to form metal−metal and $\pi-\pi$ interactions.[1−4] Such interactions have been exploited to give drastic spectroscopic changes and luminescence enhancement by polymer-induced[3a,b] or solvent-induced[3c−f] molecular association processes. Moreover, the potential of exploiting these metallophilic interactions in the development of supramolecular architectures has also been demonstrated through the self-assembly of platinum(II) polypyridine complexes to form metallogels, well-defined supramolecular morphologies and liquid crystals.[3,4]

Polyhedral oligomeric silsesquioxane (POSS) is the smallest silica nanoparticle adopting a well-defined cage-like conformation with a highly rigid silica core surrounded by multiple tunable organic substituents,[5] which determine the properties of the molecules including reactivity, solubility, thermal stabilities, and mechanical properties as well as other physical properties.[6] Moreover, these peripheral groups allow specific interactions among POSS molecules or with other molecules in the medium, which facilitate the utilization of incompressible rigid POSS cores as nanobuilding blocks toward self-assembly into distinct supramolecular architectures,[7a,b] gels,[7c] and liquid crystals.[7d] Owing to their well-defined nanostructures, together with their readily functionalized substituents, POSSs have widely been employed to create hybrid materials with precisely controlled nanostructures and properties.[7e−g]

Despite the extraordinary properties provided by organosilanes, the use of transition-metal-coordinated organosilane monomeric precursors toward supramolecular self-association has not been extensively explored. In view of the rich photophysical properties of the square-planar d^8 platinum(II) terpyridine system and their propensity toward the formation of Pt···Pt and $\pi-\pi$ interactions,[1−4] it is anticipated that such interactions, together with the incorporation of hydrophobically modified POSS, could provide additional driving forces for the self-assembly processes. Moreover, owing to their rich photophysical properties, it is envisaged that the formation of such supramolecular nanostructures could lead to interesting spectroscopic and luminescence changes, which could serve as a reporter for the formation of supramolecular assemblies. Herein we report the synthesis and characterization of the POSS-functionalized alkynylplatinum(II) terpyridine complexes (Scheme 1) and their self-assembly behaviors to form nanoscaled

Scheme 1

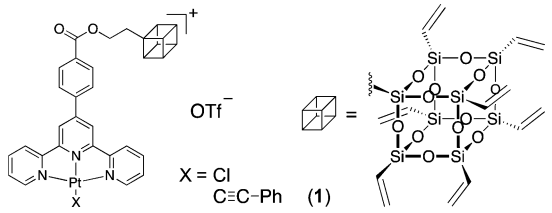

superstructures. The associated spectroscopic and luminescence changes in various solvent compositions have also been explored. In addition, the crystal structure of the chloroplatinum(II) precursor complex has been determined by X-ray crystallography.

The perspective view of the complex cation of the chloroplatinum(II) precursor complex reveals that the platinum(II) terpyridine moiety is linked to the heptavinyl POSS moiety through an ester linkage (Figure 1a and Supporting Information (SI), Figure S1a). Crystallographic and structural refinement data are given in SI, Table S1. The platinum(II) atom is in a distorted square-planar geometry, and the deviation of the *trans*-N−Pt−N bond angle from 180° [N(1)−Pt(1)−N(3)

Received: September 30, 2014
Published: December 19, 2014

dx.doi.org/10.1021/ja510048b | *J. Am. Chem. Soc.* 2014, 136, 17910−17913

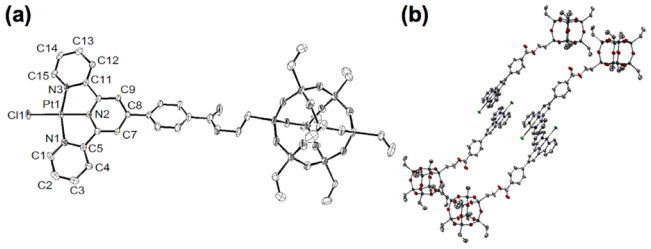

Figure 1. (a) Perspective drawing of the complex cation of [Pt(tpy-C_6H_4-VPOSS)Cl]OTf. Hydrogen atoms, counteranions, and solvent molecules are omitted for clarity. Thermal ellipsoids were shown at the 30% probability level. (b) Crystal-packing diagrams of the complex cations showing a head-to-tail configuration for the dimeric structure.

161.7(2)°] (SI, Table S2) is due to the restricted bite angle of terpyridine, which has been commonly observed in other related platinum(II) terpyridine complexes.[2a−c,3c] The crystal packing diagram shows that the cationic molecules are stacked in a head-to-tail configuration (Figures 1b and S1b), as revealed by the rotation of the individual molecules with respect to their neighbors with a C−Pt−Pt−C torsional angle of 180°, such that the POSS moieties are packed in close proximity, suggesting the propensity of the POSS moieties to pack or aggregate in an ordered manner. The Pt···Pt distance is found to be 3.35 Å within the dimeric structure, indicating the presence of significant Pt···Pt interactions.

Dissolution of **1** in pure tetrahydrofuran (THF) gives a clear yellow solution that shows high- and low-energy absorption bands in the UV−vis absorption spectrum, as shown in Figure 2;

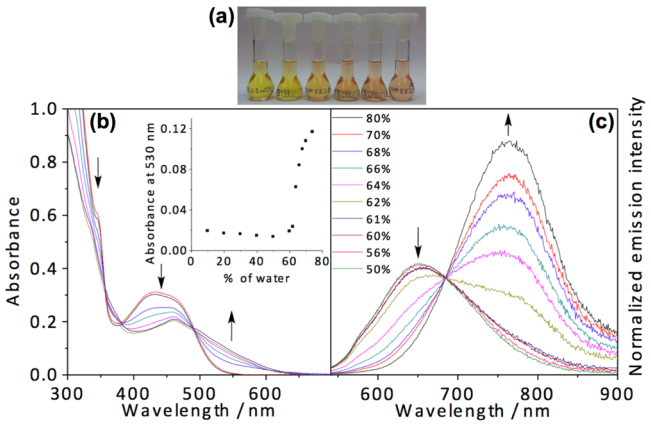

Figure 2. (a) Solutions of **1** in THF−water mixture (percentage of water in THF from left to right: 60, 62, 64, 66, 68, 70%). (b) UV−vis absorption spectra of **1** in THF with increasing water content from 60 to 74%. (c) The corresponding corrected emission spectral changes normalized at 685 nm upon increasing the water composition from 50 to 80%.

the corresponding photophysical data are summarized in SI, Table S3. With reference to our previous work on alkynylplatinum(II) terpyridine complexes,[2c,3a,c−e] the high-energy absorption band at ca. 280−350 nm is assigned to the intraligand (IL) [$\pi\rightarrow\pi^*$] transitions of alkynyl and terpyridine ligands, while the low-energy absorption band at ca. 400−490 nm is assigned to the metal-to-ligand charge-transfer (MLCT) [$d\pi(Pt)\rightarrow\pi^*(tpy)$] transition mixed with an alkynyl-to-terpyridine ligand-to-ligand change-transfer (LLCT) character. The low-energy absorption bands at ca. 450 nm in the concentration range of 40−110 μM are found to obey Beer's law (SI, Figure S2), indicating that there is no significant occurrence of complex aggregation in THF. Notably, this complex would exhibit strong solvatochromism upon the increase of water content in THF solution (Figure 2a, [Pt] = 40 μM). The solution color of **1** is found to change from yellow (100% THF) to red (70% H_2O), accompanied by a new absorption shoulder at ca. 560 nm with clear isosbestic points in the UV−vis absorption spectral traces, as depicted in Figure 2b. The newly formed absorption shoulder is typically assigned to metal−metal-to-ligand charge-transfer (MMLCT) transitions, brought about by the Pt···Pt and/or $\pi-\pi$ interactions as a result of hydrophobic interactions of the alkynylplatinum(II) terpyridine and POSS moieties upon the increase in solvent polarity.[3a,c−e] The corresponding plot of the absorbance at ca. 530 nm versus water content (Figure 2b, inset) reveals that a critical water content of around 62% is required to trigger the growth of the MMLCT transition band, demonstrating the formation of metal−metal interactions. Concomitant with the observation in the UV−vis absorption traces of **1**, a drop of the ^{3}MLCT/^{3}LLCT emission band at 650 nm, together with an emerging NIR luminescence at 765 nm, is observed upon increasing water content in the THF solution (Figure 2c, S3). Such red-shifted and enhanced luminescence at high water content could be attributed to the presence of Pt···Pt and $\pi-\pi$ stacking interactions as a result of the increased solvent polarity that would induce the self-assembly, further supporting the formation of aggregates driven by metallophilic and hydrophobic interactions upon an increase in the solvent polarity. In stark contrast to **1**, the poor solubility of the chloroplatinum(II) precursor complex has essentially prohibited the spectroscopic and aggregation studies, illustrating the significance of the alkynyl moiety in enhancing the solubility.

Further support came from the ^{1}H NMR experiments at various THF−water compositions (Figure S4), revealing that **1** would undergo the aggregation process in aqueous media. Well-resolved proton signals with chemical shifts and splitting patterns consistent with the chemical formulation are observed in the 20% water−THF mixture. Further increasing the water composition to 60% would result in an upfield shift and a broadening of the signals corresponding to the terpyridine and POSS moieties, suggestive of the presence of molecular interactions in the self-assembly process at higher water content.

To verify the identity of the aggregate species for the organosilane hybrids in such environments, electron microscopies and dynamic light scattering (DLS) have been employed to understand the assembly process and the spectral changes observed in the UV−vis absorption, emission, and NMR experiments. Interestingly, TEM and SEM images of **1** in 30% water in THF solution show ring-like nanostructures with internal and external diameters of ca. 100 and 300 nm respectively (Figure 3a,b). Subsequent AFM (Figure 3c) and DLS (SI, Table S4) measurements on **1** have also been made to confirm the presence of discrete nanorings with heights of ca. 40 nm and hydrodynamic diameters of ca. 709 nm under the same condition. Upon the addition of water to 70%, the solution would turn red, and this has been accompanied by the formation of nanorods of ca. 20 nm wide and lengths of a few hundred nm as revealed in the corresponding TEM and SEM images (Figure 3d,e). Similar nanorod-like structures could also be illustrated by means of AFM, which indicates the height of the nanorods to be ca. 15 nm (Figure 3f). Preliminary estimation based on the above electronic micrographs as well as the calculated molecular dimensions derived from X-ray crystallography studies, suggested that these nanorods could probably adopt a multilayer

dx.doi.org/10.1021/ja510048b | J. Am. Chem. Soc. 2014, 136, 17910−17913

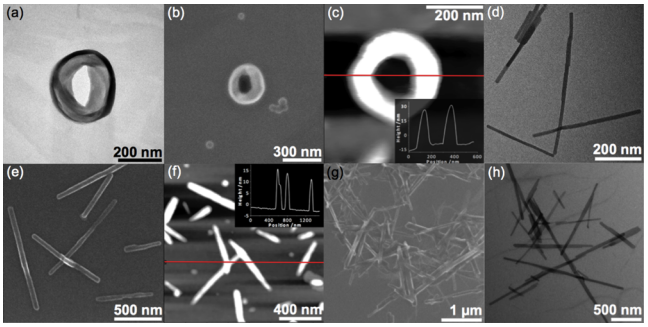

Figure 3. TEM, SEM, and AFM images of the superstructures prepared from **1** (2×10^{-4} M) in (a–c) 30% and (d–f) 70% water–THF mixture. Inset: Height profile of the nanostructures at the selected cross-section (indicated as red line). (g) SEM and (h) TEM images of the superstructures prepared from **1** (2×10^{-4} M) in 40% hexane–THF mixture.

linear configuration. The formation of these well-defined nanostructures derived from platinum-containing small molecules of organosilane hybrid is, to the best of our knowledge, unexplored. Moreover, this unprecedented transformation of the organosilane hybrids from circular rings to straight rods upon an increase in solvent polarity is believed to be related to the formation of metallophilic and $\pi-\pi$ interactions of the alkynylplatinum(II) terpyridine moiety, as revealed from the MMLCT absorption shoulder and emission band in the UV–vis and emission spectra, respectively. The metal-free terpyridine organic counterpart with solely $\pi-\pi$ stacking and hydrophobic interactions showed no well-defined nanostructures under similar conditions. This absence of well-defined morphologies in the organic counterpart has revealed the importance of the platinum(II) metal center which promoted the planarization of the terpyridine moieties through their coordination, facilitating the formation of $\pi-\pi$ stacking and Pt···Pt interactions toward the formation of supramolecular architectures, although the role of counterions in the aggregation could not be excluded.

From the electronic micrographs and the other spectroscopic changes observed, together with the consideration of the hydrophobicity of the POSS as well as the alkynylplatinum(II) terpyridine moieties, a proposed mechanism for the aggregation process is suggested as depicted in Figure 4. In pure THF, complex **1** would be well solvated without significant ground-state aggregation. However, upon the slight increase in water content to 30%, the POSS nanocages functionalized with hydrophobic vinyl groups would start to avoid unfavorable contact with the aqueous media. They would undergo self-assembly into ring-like scaffolds, appended with alkynylplatinum(II) terpyridine moieties at the exterior. At this solvent composition, no significant Pt···Pt and $\pi-\pi$ stacking interactions are observed in the UV–vis and emission spectra, suggesting that the less hydrophobic, cationic-charged alkynylplatinum(II) terpyridine moiety is still solvated and well dispersed. However, the configuration of the nanorings would have a profound impact when the polarity of the solvent is further increased. Once the water content has reached ca. 70%, the alkynylplatinum(II) terpyridine complexes appended on the aggregated nanocubes would associate into closer proximities with the formation of Pt···Pt and $\pi-\pi$ stacking interactions, which give rise to the appearance of the new MMLCT absorption and emission bands as well as the broadening of the ^{1}H NMR signals. Such molecular association governed by metal complexes would provide the directional metallophilic interactions, which

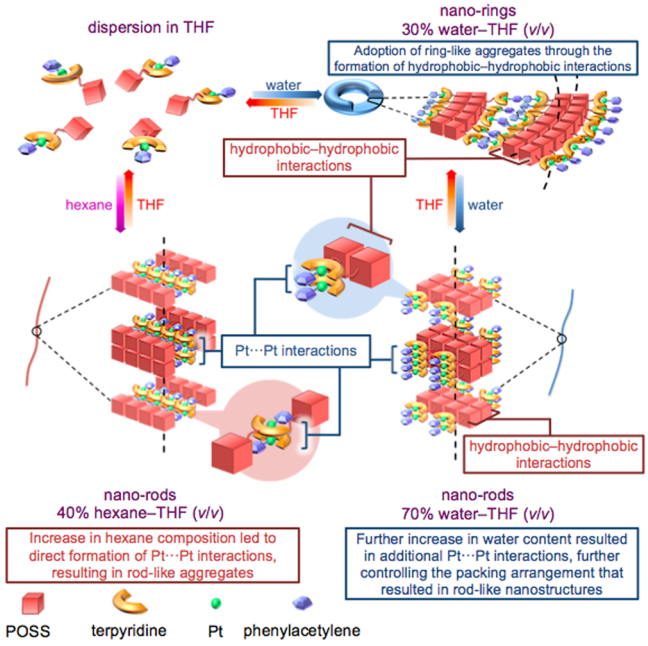

Figure 4. Schematic drawing of the morphological transformation of **1** in THF with varying solvent compositions.

further limit the packing arrangement of the aggregated species into a head-to-head manner. With the alignment of the metallophilic interactions of the alkynylplatinum(II) terpyridine complexes, the POSS organosilane hybrids would gradually transform into linear rods from circular rings upon an increase in the solvent polarity. To further support this proposed transformation, the TEM of complex **1** at 50% water in THF mixture has been conducted, showing that the generation of the rod is evolved from the ring (SI, Figure S5). The presence of both directional interactions gradually controls the packing conformations and contributes to the morphological transformation, which is not commonly achievable in the pure organic counterpart with solely $\pi-\pi$ stacking or hydrophobic–hydrophobic interactions.

To further investigate the effect of solvent polarity toward the self-association behaviors of the complexes, their aggregation behaviors are also investigated in nonpolar solvent mixtures. It is interesting to note that the yellow solution of **1** in THF (100%) would turn red upon raising the hexane content to 40%, as revealed from the UV–vis absorption changes in SI, Figure S6a and luminescence changes in SI, Figure S6b, similar to that demonstrated in the corresponding THF–water mixtures. This reveals the presence of ground-state self-association, accounting for the phenomenon that the poor solvent would induce the self-assembly of the alkynylplatinum(II) terpyridine complexes with the formation of metallophilic interactions which directly results in nanorods. The corresponding TEM and SEM images at 40% hexane–THF mixture show rod-like aggregates with lengths of a few μm and widths of about 30 nm (Figure 3g,h), indicating that the self-assembly processes proceed not only in polar medium but also in nonpolar solvents.

In contrast to the self-assembly behaviors demonstrated in polar medium, the increase in nonpolar solvent could probably result in better solvation of the hydrophobic POSS moieties while the positively charged platinum(II) terpyridine moiety would become less solvated upon increasing the nonpolar solvent content. The poorly solvated platinum(II) moieties

dx.doi.org/10.1021/ja510048b | J. Am. Chem. Soc. 2014, 136, 17910–17913

would be forced to pack together through Pt···Pt and $\pi-\pi$ stacking interactions to limit further unfavorable interactions with the nonpolar media whereas the hydrophobic POSS groups are well dispersed in hexane medium and surrounding the platinum(II) complexes to form nanorods as illustrated in Figure 4. The reduction in solvation would promote the aggregation of the platinum(II) terpyridine moieties, which would subsequently lead to the formation of Pt···Pt and $\pi-\pi$ stacking interactions, resulting in a ground state association of the molecules into a head-to-tail conformation similar to that found in the X-ray crystal structure.[8] Such formation of non-covalent interactions would account for both the colorimetric and morphological changes.

To conclude, an alkynylplatinum(II) terpyridine complex functionalized with POSS moieties has been reported, which demonstrated the capability to form various distinct morphologies that can be systematically controlled by the variation of solvent polarity. Such self-association process is governed by the formation of Pt···Pt and $\pi-\pi$ stacking interactions as well as the hydrophobic interactions provided by the POSS moieties. The interesting morphological transformation from nanorings to rod-like nanostructures in various solvent media, which is associated with spectroscopic changes, has been demonstrated by UV−vis absorption, emission studies, and the electronic micrographs. The present study illustrates that the incorporation of platinum(II) complexes into organosilane moieties would open up a new strategy to construct various nanostructures in organosilane hybrids, serving as potential candidates in the development of a new class of functional supramolecular materials.

■ ASSOCIATED CONTENT

Supporting Information

Synthetic procedures, characterization data, 1D NMR and NOESY data, X-ray crystallography data, DLS data, and UV−vis spectroscopic data. This material is available free of charge via the Internet at http://pubs.acs.org.

■ AUTHOR INFORMATION

Corresponding Author

wwyam@hku.hk

Notes

The authors declare no competing financial interest.

■ ACKNOWLEDGMENTS

V.W.-W.Y. acknowledges support from The University of Hong Kong under the University Research Committee (URC) Strategic Research Theme on New Materials. This work has been supported by the University Grants Committee Areas of Excellence (AoE) Scheme (AoE/P-03/08) and a General Research Fund (GRF) grant from the Research Grants Council of Hong Kong Special Administrative Region, P. R. China (HKU 7060/12P). H.-L.A.-Y. acknowledges the receipt of a Postgraduate Studentship, and S.Y.-L.L. acknowledges the receipt of a University Postdoctoral Fellowship, both administered by The University of Hong Kong. X-ray data collection by Prof. Raymond W. Y. Wong of the Hong Kong Baptist University and the assistance by Dr. Lap Szeto in solving the crystallographic data are gratefully acknowledged.

■ REFERENCES

(1) (a) Schindler, J. W.; Fukuda, R. C.; Adamson, A. W. *J. Am. Chem. Soc.* **1982**, *104*, 3596. (b) Miskowski, V. M.; Houlding, V. H. *Inorg. Chem.* **1989**, *28*, 1529. (c) Miskowski, V. M.; Houlding, V. H.; Che, C. M.; Wang, Y. *Inorg. Chem.* **1993**, *32*, 2518. (d) Miskowski, V. M.; Houlding, V. H. *Inorg. Chem.* **1991**, *30*, 4446. (e) Kunkely, H.; Vogler, A. *J. Am. Chem. Soc.* **1990**, *112*, 5625. (f) Herber, R. H.; Croft, M.; Coyer, M. J.; Bilash, B.; Sahiner, A. *Inorg. Chem.* **1994**, *33*, 2422.

(2) (a) Jennette, K. W.; Gill, J. T.; Sadownick, J. A.; Lippard, S. J. *J. Am. Chem. Soc.* **1976**, *98*, 6159. (b) Lippard, S. J. *Acc. Chem. Res.* **1978**, *11*, 211. (c) Aldrige, T. K.; Stacy, E. M.; McMillin, D. R. *Inorg. Chem.* **1994**, *33*, 722. (d) Yam, V. W. W.; Tang, R. P. L.; Wong, K. M. C.; Cheung, K. K. *Organometallics* **2001**, *20*, 4476. (e) Yam, V. W. W. *Acc. Chem. Res.* **2002**, *35*, 555. (f) Hill, M. G.; Bailey, J. A.; Miskowski, V. M.; Gray, H. B. *Inorg. Chem.* **1996**, *35*, 4585. (g) Connick, W. B.; Marsh, R. E.; Schaefer, W. P.; Gray, H. B. *Inorg. Chem.* **1997**, *36*, 913. (h) Bailey, J. A.; Hill, M. G.; Marsh, R. E.; Miskowski, V. M.; Schaefer, W. P.; Gray, H. B. *Inorg. Chem.* **1995**, *34*, 4591.

(3) (a) Yu, C.; Wong, K. M. C.; Chan, K. H. Y.; Yam, V. W. W. *Angew. Chem., Int. Ed.* **2005**, *44*, 791. (b) Chung, C. Y. S.; Chan, K. H. Y.; Yam, V. W. W. *Chem. Commun.* **2011**, *47*, 2000. (c) Wong, K. M.-C.; Yam, V. W.-W. *Acc. Chem. Res.* **2011**, *44*, 424. (d) Yam, V. W. W.; Wong, K. M. C.; Zhu, N. *J. Am. Chem. Soc.* **2002**, *124*, 6506. (e) Yam, V. W. W.; Chan, K. H. Y.; Wong, K. M. C.; Zhu, N. *Chem.—Eur. J.* **2005**, *11*, 4535. (f) Po, C.; Tam, A. Y. Y.; Wong, K. M. C.; Yam, V. W. W. *J. Am. Chem. Soc.* **2011**, *133*, 12136. (g) Po, C.; Tam, A. Y. Y.; Yam, V. W. W. *Chem. Sci.* **2014**, *5*, 2688. (h) Po, C.; Yam, V. W. W. *Chem. Sci.* **2014**, *5*, 4868.

(4) (a) Leung, S. Y. L.; Yam, V. W. W. *Chem. Sci.* **2013**, *4*, 4228. (b) Lu, W.; Chui, S. S. Y.; Ng, K. M.; Che, C. M. *Angew. Chem.* **2008**, *120*, 4644. (c) Yuen, M. Y.; Roy, V. A. L.; Lu, W.; Kui, S. C. F.; Tong, G. S. M.; So, M. H.; Chui, S. S. Y.; Muccini, M.; Ning, J. Q.; Xu, S. J.; Che, C. M. *Angew. Chem., Int. Ed.* **2008**, *47*, 9895. (d) Tam, A. Y. Y.; Wong, K. M. C.; Wang, G.; Yam, V. W. W. *Chem. Commun.* **2007**, *20*, 2028. (e) Tam, A. Y. Y.; Wong, K. M. C.; Yam, V. W. W. *J. Am. Chem. Soc.* **2009**, *131*, 6253. (f) Kozhevnikov, V. N.; Donnio, B.; Bruce, D. W. *Angew. Chem., Int. Ed.* **2008**, *47*, 6286. (g) Lu, W.; Chen, Y.; Roy, V. A. L.; Chui, S. S. Y.; Che, C. M. *Angew. Chem., Int. Ed.* **2009**, *48*, 7621.

(5) (a) Lichtenhan, J. D. *Comments Inorg. Chem.* **1995**, *17*, 115. (b) Cordes, D. B.; Lickiss, P. D.; Rataboul, F. *Chem. Rev.* **2010**, *110*, 2081. (c) Wu, J.; Mather, P. T. *Polym. Rev.* **2009**, *49*, 25.

(6) (a) Haddad, T. S.; Lichtenhan, J. D. *Macromolecules* **1996**, *29*, 7302. (b) Mammeri, F.; Bourhis, E. L.; Rozes, L.; Sanchez, C. *J. Mater. Chem.* **2005**, *15*, 3787. (c) Moore, B. M.; Ramirez, S. M.; Yandek, G. R.; Haddad, T. S.; Mabry, J. M. *J. Organomet. Chem.* **2011**, *696*, 2676. (d) Drazkowshi, D. B.; Lee, A.; Haddad, T. S.; Cookson, D. J. *Macromolecules* **2006**, *39*, 1854. (e) Bolln, C.; Tsuchida, A.; Frey, H.; Mülhaupt, R. *Chem. Mater.* **1997**, *9*, 1475.

(7) (a) Jiang, B.; Tao, W.; Lu, X.; Liu, Y.; Jin, H.; Pang, Y.; Sun, X.; Yan, D.; Zhou, Y. *Macromol. Rapid Commun.* **2012**, *33*, 767. (b) Yu, X.; Zhong, S.; Li, X.; Tu, Y.; Yang, S.; Horn, R. M. V.; Ni, C.; Pochan, D. J.; Quirk, R. P.; Wesdemiotis, C.; Zhang, W. B.; Cheng, S. Z. D. *J. Am. Chem. Soc.* **2010**, *132*, 16741. (c) Kuo, S. W.; Lee, H. F.; Huang, W. J.; Jeong, K. U.; Chang, F. C. *Macromolecules* **2009**, *42*, 1619. (d) Cui, L.; Collet, J. P.; Xu, G.; Zhu, L. *Chem. Mater.* **2006**, *18*, 3503. (e) Sanchez, C.; Soler-Illia, G. J. A. A.; Ribot, F.; Lalot, T.; Mayer, C. R.; Cabuil, V. *Chem. Mater.* **2001**, *13*, 3061. (f) Jeon, H. G.; Mather, P. T.; Haddad, T. S. *Polym. Int.* **2000**, *49*, 453. (g) Gilman, J. W.; Schlitzer, D. S.; Lichtenhan, J. D. *J. Appl. Polym. Sci.* **1996**, *60*, 591.

(8) The crystal for X-ray structure determination was obtained from nonpolar medium. ^{1}H NMR experiments at various THF−hexane compositions (SI, Figure S7) revealed the aggregation in nonpolar medium. NOESY experiments (SI, Figures S8 and S9) showed cross-peaks between the phenyl ring and the terpyridine signals, suggesting possible head-to-tail conformation.